

## Experimental aspects of dissipation force microscopy

C. Loppacher,<sup>\*</sup> R. Bennewitz,<sup>†</sup> O. Pfeiffer, M. Guggisberg, M. Bammerlin, S. Schär, V. Barwich, A. Baratoff, and E. Meyer

*Institute of Physics, University of Basel, Klingelbergstrasse 82, CH-4056 Basel, Switzerland*

(Received 7 June 2000)

Experimental aspects of measuring dissipation on atomic scale using large-amplitude dynamic force microscopy are discussed. Dissipation versus distance curves reveal that long- and short-range forces contribute to the dissipation. The decay length of short-range contributions is found to be close to that of the tunneling current. The dependence of dissipation on the bias voltage and on the oscillation amplitude is presented. Atomic-scale lateral variations of dissipation are discussed, and the role of the atomic constitution of the tip for quantitative results is pointed out.

### I. INTRODUCTION

Force microscopy measures the forces between a nanometer-scale tip and a surface, or uses the tip-sample force as feedback for a distance control to record topography maps. During the operation dissipation takes place when a part of the work done by the forces is converted into heat. This is an important issue in friction force microscopy (FFM) where the microscopic origins of dissipation in repulsive contact are studied. In stick-slip processes, for example, a lateral force is built up while the tip sticks to an atomic site. When the tip slips to a relaxed position the stored energy is released instantaneously compared to the time scale of most experiments. The mean power dissipation  $\bar{P}$  in such experiments is the product of the mean lateral force  $\bar{F}_L$  and the scan velocity  $\bar{P} = \bar{F}_L v$ . In recent atomic-scale stick-slip experiments we have found as typical values  $\bar{P} = 1.2 \times 10^{-16}$  W on Cu(111) and  $\bar{P} = 0.2 \times 10^{-16}$  W on NaCl(100) at a scan velocity of 50 nm/s.<sup>1,2</sup> The origins of dissipation in friction are related to phonon excitations, electronic excitations, and irreversible changes of the surface.

However, dissipation also occurs in noncontact modes of force microscopy, where the atomic structure of tip and sample are reliably preserved. This type of dissipation experiment is the subject of the present study. The first experimental demonstration was reported by Denk and Pohl, who analyzed the resonance of an oscillating cantilever with a metallic tip in electrostatic interaction with a heterostructured semiconducting sample.<sup>3</sup> In this experiment, the cantilever oscillation was damped by Joule dissipation of charge carriers, which were moved by the oscillating electric field produced by the tip vibration. The authors pointed out that the damping deduced from the resonance analysis could also be obtained from the excitation amplitude needed to maintain a constant oscillation amplitude. In addition to this work, Stowe *et al.* recently demonstrated the dependence on bias voltage, dopant concentration, and tip-sample distance of electrostatic damping close to a semiconducting surface.<sup>4</sup> Lüthi *et al.* were the first to present data of atomic-scale variation of dissipation in a noncontact dynamic force microscope on a Si(111)  $7 \times 7$  surface, where the strongest damping was found at the sites of the corner holes.<sup>5</sup>

The distance dependence of dissipative forces has been studied by Gotsmann *et al.*, who found dissipation in the picowatt range when a silicon tip comes into close proximity to a mica surface.<sup>6</sup> These authors discuss simple models for evaluation of the power that are tested with the help of numerical simulations and compared to experimental results.

The origins of dissipation in noncontact force microscopy are still under discussion. While the explanation of long-range electrostatic damping by Joule dissipation is well established and experimentally justified,<sup>3,4</sup> short-range contributions on the atomic scale are less understood. Lüthi *et al.* speculated about coupling of forces exerted on surface atoms into low-frequency modes of the phonon bath.<sup>5</sup> A molecular dynamics simulations of dynamic force microscopy on Si(111)  $7 \times 7$  by Abdurixit *et al.* revealed that the response of surface atoms to the force exerted by the approaching tip is partially nonadiabatic despite the quasistatic movement of the tip on the atomic time scale.<sup>7</sup> The power dissipation connected with the nonadiabatic response was found to depend quadratically on the respective interaction force. Recently, Gauthier and Tsukada presented a calculation of dissipation in the tip-sample interaction due to thermal fluctuations even for a fully adiabatic approach of the tip towards the surface.<sup>8</sup> In this model, dissipation is essentially proportional to the square of the force gradient, and to the square root of the oscillation amplitude. Based on their results the authors suggest to use dissipation as feedback parameter for a new type of force microscopy that would circumvent certain problems of dynamic force microscopy arising from long-range forces. The characteristics of a dissipation feedback would be closer to tunneling microscopy than to conventional dynamic force microscopy (DFM) regulated to constant frequency shift. Actually, such an experiment has already been realized by Jarvis *et al.*, who in their report emphasize the monotonic increase of dissipation as an advantage for the distance regulation compared to the nonmonotonic trend of frequency with distance.<sup>9</sup>

In this paper, we first describe how we measure dissipation with a dynamic force microscope. Experimental results for the dependence of dissipation on distance, bias voltage, and oscillation amplitude are presented. The lateral resolution of dissipation measurements and its dependence on the tip constitution is discussed based on new results for the

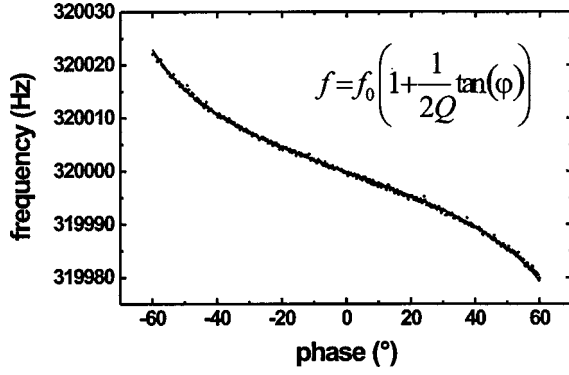


FIG. 1. Determination of the quality factor of the cantilever oscillation in a phase variation experiment. The frequency shift of the constant amplitude oscillation reveals a quality factor of 12 800.

Si(111)7×7 and the KBr(100) surface.

## II. EXPERIMENT

In our study we used a noncontact atomic-force microscope (AFM) in the constant-amplitude mode, implemented in a ultrahigh-vacuum chamber. This technique has been described in detail elsewhere.<sup>10</sup> To summarize, the tip is oscillating with a constant amplitude  $A$  of typically 1–10 nm at the eigenfrequency  $f$  of the cantilever, which may shift by  $\Delta f$  due to forces between tip and sample. The oscillation amplitude is kept constant by a regulation circuit that excites a piezoactuator with a sinusoidal voltage of the oscillation frequency  $f$  and an amplitude  $V_{exc}$ . The actuator shakes the fixed end of the cantilever. When the cantilever oscillation is damped due to the tip-sample interaction,  $V_{exc}$  will increase to maintain the oscillation amplitude constant. By recording  $\Delta f$  and  $V_{exc}$  simultaneously, forces and dissipation can be measured. The frequency tracking and amplitude control in our experiment is done by a homebuilt digital device including a phase-locked loop.<sup>11</sup>

In all dynamic force microscopy measurements the power dissipation  $P_0$  caused by internal friction in the freely oscillating cantilever is given by

$$P_0 = 2\pi f_0 \frac{\frac{1}{2} k A^2}{Q}, \quad (1)$$

with  $f_0$  the eigenfrequency of the freely oscillating cantilever,  $k$  its spring constant, and  $Q$  the quality factor of the oscillation. This dissipation is independent of the sample and cannot be avoided; it produces a background signal in which

variations of the dissipation have to be detected. Therefore, measurements with small oscillation amplitudes are highly desirable for dissipation force microscopy. The spring constant  $k$  is calculated from the geometrical dimensions of the cantilever and its eigenfrequency. Spring constants and oscillation amplitudes can be determined within an error of 10%, resulting in an error of about 25% for all absolute values of power dissipation given below. The quality factor  $Q$  can be easily determined in a digitally controlled phase variation experiment as shown in Fig. 1.

The extra dissipation  $P_{ts}$  caused by tip-sample interaction can be calculated from  $V_{exc}$  according to<sup>6</sup>

$$P_{ts} = P_0 \left( \frac{V_{exc}}{V_{exc,0}} - \frac{f}{f_0} \right), \quad (2)$$

where  $V_{exc,0}$  is the excitation voltage needed to maintain the oscillation amplitude far from the surface. Since frequency shifts in our experiments never exceed the order of  $10^{-3}$  of the resonance frequency we can always set  $f/f_0 = 1$ .

## III. RESULTS

### A. Dissipation versus distance curves on Cu(111)

In order to reveal the nature of dissipation in dynamic force microscopy experiments we have simultaneously recorded the frequency shift, the dissipation, and the tunneling current as a function of distance during approach to the surface. Two series of measurements are presented here: *Series I* consists of distance curves recorded at systematically varied bias voltages, *Series II* of distance curves using varied oscillation amplitudes. The parameters used in the two series are given in Table I together with a description of the tip preparation, which is important for these measurements as discussed below. The experiments were performed on clean, atomically flat copper surfaces. In order to avoid repulsive contacts with irreversible changes of tip and surface and to ensure reproducible results even in the short-range regime we have stopped the tip approach when certain threshold values of either the tunneling current or  $V_{exc}$  were reached. In this way even atomic-scale changes of the tip structure can be widely excluded.

In Fig. 2, two dissipation versus distance curves from series I are plotted, recorded at sample bias voltages of  $U_{bias} = 0.9$  V and  $U_{bias} = 0.0$  V. Both curves show a steep, congruent increase of dissipation on the last nanometer before the approach is stopped. At distances larger than 1 nm away from the stopping point, however, an additional long-range contribution is found for the curve recorded at  $U_{bias} = 0.9$  V.

TABLE I. Parameters and results of series I and series II.

	Series I	Series II
Parameter varied	Amplitude $A$	Bias voltage $U$
Resonance frequency $f_0$	147 785 kHz	319 254 kHz
Spring constant $k$	21 N/m	22.6 N/m
$Q$ factor	12 800	15 000
Tip constitution	Covered by Cu after prolonged scanning in contact mode	Oxide layer removed from the silicon tip by argon-ion sputtering
Contact potential difference to Cu(111)	−0.08 V	−0.97 V

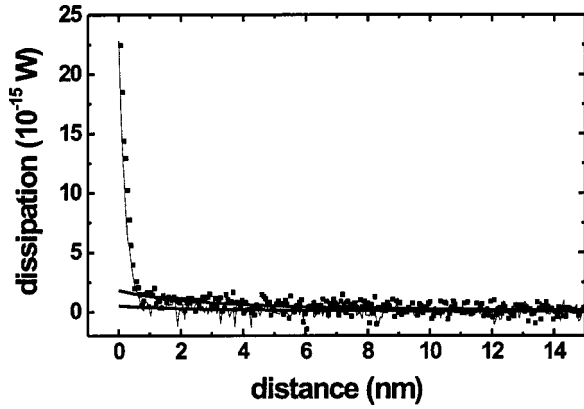


FIG. 2. Power dissipation vs distance for  $U_{bias} = 0.9$  V (squares) and  $U_{bias} = 0.0$  V (thin line) ( $f_0 = 147785$  Hz,  $k = 21$  N/m,  $A = 8.8$  nm,  $P_0 = 5 \times 10^{-14}$  W). The long-range part of the dissipation has been fitted with the function  $\Delta P = c/(z - z_0)^2$  as indicated by the two thick lines.

This long-range part of all dissipation curves of series I has been fitted with a function  $P = c/(z - z_0)^2$ . The offset  $z_0$ , which is identical in all fits, reflects the fact that the mesoscopic tip is the source of electrostatic long-range interactions, while the end of a nanotip with height  $z_0$  causes the short-range forces.<sup>10</sup> Using the parameters of these fits, the dissipation at a distance of 1 nm is plotted in Fig. 3 together with the similarly determined long-range contribution of the frequency shift, the latter being a measure for the mean long-range force. Both the frequency shift and the dissipation show a quadratic dependence on the sample bias. This finding indicates that the electrostatic contributions to force and dissipation are proportional to each other. However, the minima of both curves are not zero but have a certain offset value. The offset of the frequency shift can be easily explained by van der Waals forces, which are always present independent of the bias voltage. The existence of the long-range dissipation at the minimum of electrostatic forces may be due to remaining electrostatic forces that cannot be completely eliminated, since the complicated geometrical and chemical structure of the tip forecloses a well-defined contact potential.

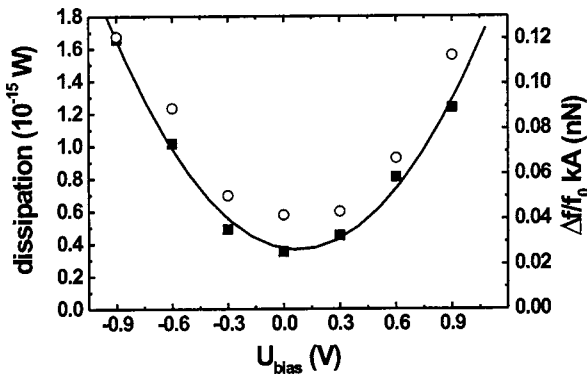


FIG. 3. Dissipation (solid squares) and normalized frequency shift (open circles) at  $z = 1$  nm. The values are the result of an analysis of the long-range contribution to the power dissipation as indicated in Fig. 2. The solid line is a parabola fitted to the dissipation data.

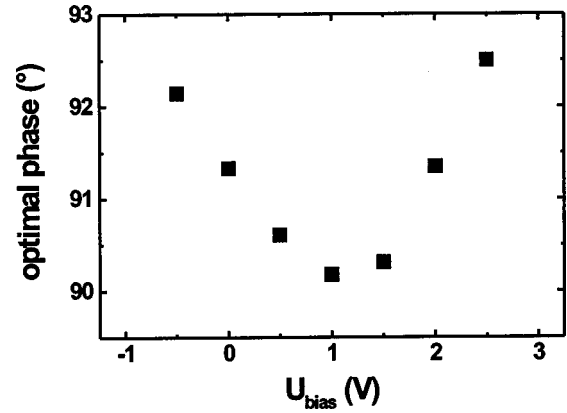


FIG. 4. Results of a phase variation experiment performed 1 nm from the surface. The phase between cantilever oscillation and excitation resulting in the lowest value of  $V_{exc}$  is plotted as a function of the sample bias. The minimum is shifted with respect to Fig. 3 due to a different contact potential of the tip (see text).

The electrostatic dissipation may be described by a phase shift between the tip oscillation and the force oscillation due to the creation of dissipating currents in the silicon tip, similar to a description of the phase shift in intermittent-contact force microscopy.<sup>12</sup> The phase shift would be zero for purely conservative forces. If the tip velocity is given by  $v(t) = \omega A \cos(\omega t)$  and the force oscillation by  $F(t) = F_\omega \sin(\omega t + \Delta\varphi)$ , the mean power dissipation would be

$$P = \frac{\omega}{2\pi} \int_0^{2\pi/\omega} F(t)v(t)dt = -\frac{1}{2} \omega A F_\omega \sin(\Delta\varphi). \quad (3)$$

In the perturbation approximation the frequency shift is related to the first Fourier coefficient  $F_\omega$  by<sup>10,13</sup>

$$F_\omega = \frac{\Delta f}{f_0} k A, \quad (4)$$

the quantity also plotted in Fig. 3. Evaluating Eq. (3) with numbers from Fig. 3 we would expect a phase shift of  $\Delta\varphi = 1.2^\circ$  at  $U_{bias} = -0.9$  V. A value in the same order of magnitude was indeed found in a phase variation experiment. In this type of measurement, the minimum of  $V_{exc}$  as a function of the phase between cantilever oscillation and excitation is determined. For the freely oscillating cantilever this optimal phase is  $90^\circ$ . Close to the surface, the optimal phase may shift due to dissipative forces. In Fig. 4 this phase is plotted as a function of the sample bias. The optimal phase is shifted away from  $90^\circ$  when the bias voltage is different from the contact potential difference. For a shift of 0.9 V a phase shift of about  $1^\circ$  can be read from Fig. 4. Note that this experiment was done with a different tip having a different contact potential difference to the copper surface and that therefore the minimum of electrostatic forces is shifted by about 1 V. However, the spring constant and eigenfrequency of the cantilever were the same as in the experiment plotted in Fig. 3, making the results comparable. The voltage-dependent shift of the phase exhibits the same distance dependence as the electrostatic interactions.

After subtraction of the long-range contributions from frequency shift and dissipation one can determine the decay

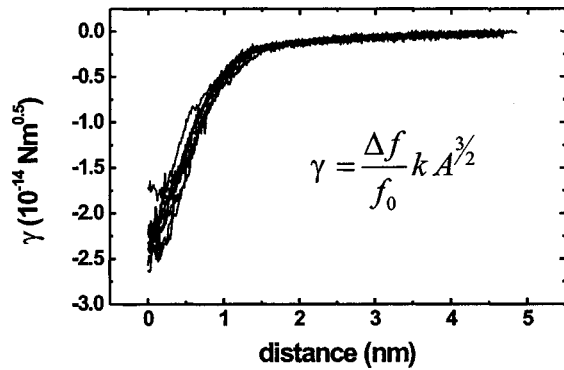


FIG. 5. Reduced frequency shift  $\gamma$  vs tip-sample distance for nine different oscillation amplitudes ( $f_0=319\,254$  Hz,  $k=22.6$  N/m,  $A=8.2$  to  $22.9$  nm,  $Q=12\,800$ , contact potential difference between tip and sample was compensated). The approach of the tip was stopped when a tunneling current of more than  $10$  pA was collected. This stopping point of the approach curve defines the distance zero. The scaling of the frequency shift with the amplitude  $\Delta f \propto A^{3/2}$  is well confirmed.

length of the short-range contribution as suggested by Guggisberg *et al.*<sup>10</sup> The decay length of the frequency shift, which is equal to the decay length of the force, varies from  $0.33$  to  $0.45$  nm and the decay length of the dissipation from  $0.21$  to  $0.28$  nm. However, the ratio between the two decay lengths is always  $1.5$ . In a previous study we found that the decay length of the force is always twice as large as the decay length of the tunneling current.<sup>14</sup>

In a second series of measurements, we compare approach curves recorded with varying oscillation amplitudes  $A$ . In these measurements the contact potential difference between tip and sample has been compensated by applying the respective bias voltage in order to minimize electrostatic forces. Figure 5 shows the force curves using the reduced frequency shift introduced by Giessibl,<sup>13</sup> which takes into consideration the well-confirmed  $A^{-3/2}$  dependency of the frequency shift and allows comparison of force measurements performed with different parameters. For comparison, the reduced frequency shift curve at  $U_{bias}=0.0$  V of the experiment of series I is added to the graph. Apart from a slightly larger long-range force due to the imperfectly compensated contact potential difference, the two tips experience rather similar forces. The power dissipation curves for varying oscillation amplitudes are shown in Fig. 6. As expected

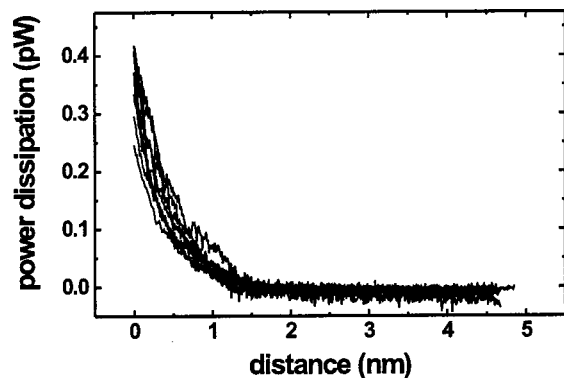


FIG. 6. Power dissipation vs distance for the measurements described in Fig. 5.

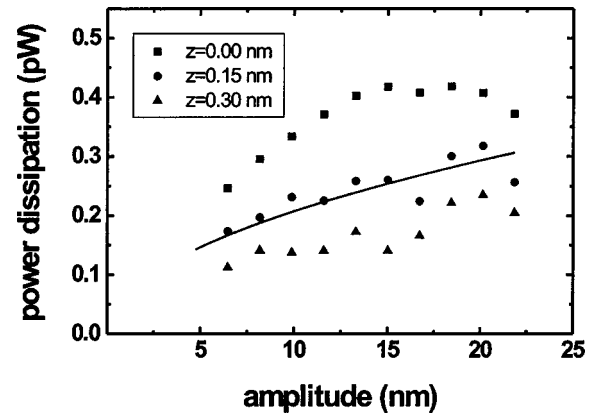


FIG. 7. Cross sections through the data plotted in Fig. 6 at different tip-sample distances. The solid line represents a square root function.

at compensated contact potential difference, significant dissipation occurs only in the short-range regime. The power dissipation is much lower than that in the variable bias voltage experiment even though the forces acting on the tip are comparable as shown in Fig. 5. To elucidate the amplitude dependence of the dissipation, cross sections through the approach curves are shown in Fig. 7. There is a clear increase of dissipation with increasing oscillation amplitude, possibly proportional to the square root of the amplitude as suggested in the models of Gotsmann *et al.*<sup>6</sup> and Gauthier and Tsukada.<sup>8</sup>

## B. Dissipation maps

In a recent publication we have presented images of a Cu(100) surface showing atomic contrast in topography and  $V_{exc}$ .<sup>14</sup> The contrast in  $V_{exc}$  being very weak, we suspect that it is formed predominantly by a convolution between the topography and the general distance dependence of the dissipation as plotted in Fig. 6. Consequently, there is no direct proof that the dissipation process exhibits variations on the atomic scale, although the contrast is caused by an atomic-scale variation of the tip-sample interactions.

On the larger Si(111)7 $\times$ 7 superstructure, we were able to record atomic-scale variations of the dissipation at constant height, where any artifacts arising from the topography variation are circumvented. In Fig. 8 the lower third of the frame shows topography, frequency shift, and dissipation while the tip-sample distance is regulated to a constant tunneling current. At the sites of the corner holes the highest frequency shift and the strongest dissipation are detected as reported previously.<sup>5,15</sup> In the upper part of the frames, the regulator is stopped and the tip is scanned at constant height, therefore without contrast in topography. Frequency shift and dissipation retain an atomic-scale contrast, demonstrating that there is a true atomic-scale variation of force and dissipation. Furthermore, the characteristic appearance of the unit cells is retained unchanged, where strongest dissipation occurs upon oscillation of the tip above a corner hole site, causing a power loss of the same order as reported in Ref. 5. In the course of scanning without regulation, the tip drifts towards the surface causing an increase of dissipation and a decrease of the negative frequency shift. The latter is in



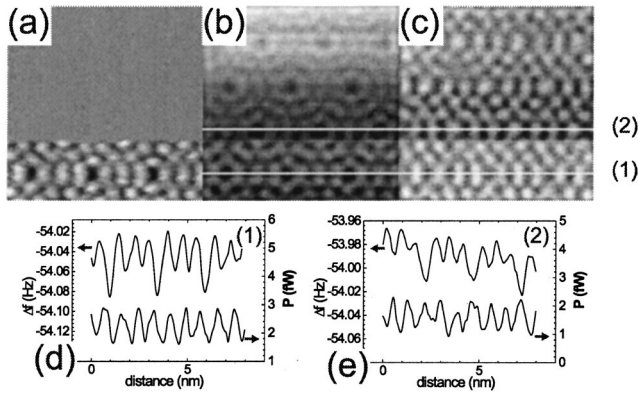


FIG. 8. (a) Topography, (b) frequency shift  $\Delta f$ , and (c) dissipation measured on a Si(111)7 $\times$ 7 surface. In the lower third of the frame, the tip-sample distance was regulated to constant tunneling current, then the regulator was switched off in order to scan at constant height. Cross sections of the frequency shift and of the dissipation before and after switching off the regulator are plotted in (d) and (e). The experimental parameters were  $\bar{I}_t=48$  pA,  $f_0=160\,322$  Hz,  $A=8.8$  nm,  $k=28.5$  N/m,  $U_{bias}=2$  V, and  $Q=15\,700$ .

agreement with our assumption that in these experiments the tip is in a regime close to the surface, where the negative frequency shift decreases with decreasing distance. The dissipation contrast observed in Fig. 8 is inverted with respect to the finding of Abdurixit *et al.*, who found strongest dissipation not at the corner holes but on top of adatoms.<sup>7</sup> However, the authors in their simulation considered only attractive chemical forces, while in this experiment all kind of interactions contribute, possibly in part repulsive as pointed out above.

A strong atomic-scale dissipation contrast at step edges has been demonstrated in a recent study by Bennewitz *et al.*<sup>16</sup> Altogether, we conclude that DFM is able to detect dissipation in the tip-sample interaction with atomic resolution. However, we would like to point out that quantitative results depend critically on the state of the tip. In previously published work on NaCl/Cu(111) (Ref. 16) and on Cu(100) (Ref. 14) we discussed the effects of slight tip changes in atomically resolved images. While the topography is hardly affected except for a change of corrugation height, the dissipation can exhibit dramatic changes and even disappear. Similar effects are demonstrated in Fig. 9. A KBr(100) surface has been imaged after irradiation with low-energy electrons. The typical topography of such a surface with monatomic cleavage steps and rectangular holes of one atomic layer depth has been described by Such *et al.*<sup>17</sup> Here, we focus on the appearance of step edges in the dissipation maps before and after a tip crash. While the topographic images show comparable contrast at the monatomic steps sites, a dissipation contrast at the step edges arises only after the tip crash. While an enhanced interaction at step sites of ionic crystals is well understood in terms of the lower coordination of edge ions, it is surprising that the energy dissipated in the tip-step interaction depends so much on the tip constitution. As a hypothesis we suggest that the tip picked up some adatoms in the crash, which may jump forth and back when the tip enters in the strong force field of the step edges, while the tip stays stable above the terraces. Such instabilities of the tip

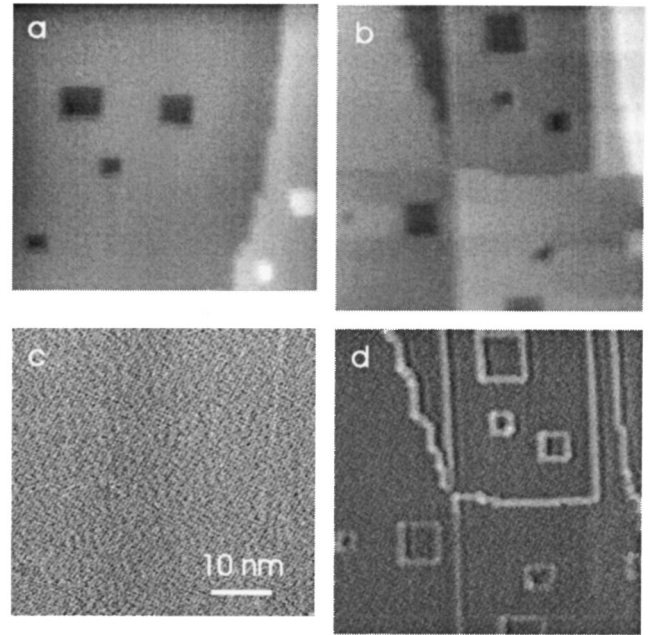


FIG. 9. (a,b) Topography and (c,d) dissipation map of a KBr(100) surface irradiated with electrons. The surface shows monatomic cleavage steps and rectangular holes and islands characteristic for electron-beam damage. Images (a,c) and (b,d) are recorded on the same sample in close vicinity, the only difference between both measurements being a tip crash, which occurred after finishing frames (a,c).

configuration could easily explain an increased dissipation in strong force field of the step edges. They would be comparable to the stick-slip processes observed in friction force microscopy. The higher dissipation found in dynamic force microscopy compared to friction force microscopy is caused by the high frequency of the cantilever oscillation, which sums up the dissipation of atomic processes in each cycle.

#### IV. CONCLUSION

Dissipation force microscopy is a promising new member of the family of scanning probe microscopes. It has proven its ability to detect dissipation processes at surfaces with true atomic resolution, especially at nonregular sites. The experimental results presented here can be summarized as follows: Dissipation in the tip-sample interaction occurs due to both short- and long-range forces, the latter being at least partly of electrostatic nature. Proportional to the mean electrostatic force, the long-range dissipation grows quadratically with the voltage applied between tip and sample and can be minimized by compensating the contact potential difference. A simple description of the electrostatic dissipation taking into account the phase delay between tip and force oscillation could be experimentally confirmed. It suggests a possible direction for a more detailed model of the dissipation measurement.

The short-range contribution to the dissipation decays exponentially with distance. The decay length is found to be larger than that of the tunneling current but shorter than that of the short-range force. The relation between force decay and dissipation decay agrees reasonably with the predictions of Abdurixit *et al.*<sup>7</sup> and Gauthier and Tsukada.<sup>8</sup> The dissipation

pated power is found to increase with increasing oscillation amplitude, in agreement with models that predict  $P \propto \sqrt{A}$ .<sup>6,8</sup>

A remaining experimental problem of dissipation force microscopy is its strong dependence of quantitative results on the tip configuration. For example, the power dissipation in the experiment described in Fig. 6 is about an order of magnitude higher than that in the experiment described in Fig. 2, both measurements being performed on clean copper surfaces. Although part of this difference can be attributed to the difference in oscillation frequency, one has to keep in mind that the tips have a different chemical constitution as manifested in the contact potential difference. The crucial role of the atomic-scale shape and chemical constitution of the tip is impressively demonstrated by the effects of tip

crashes on the dissipation measurements. Reproducible measurements of dissipation that allow comparison with atomistic models require atomically defined tips. Such tips could be prepared and controlled by *in situ* methods such as field emission<sup>18</sup> or by use of chemically well-defined structures such as carbon nanotubes.<sup>19</sup>

#### ACKNOWLEDGMENTS

This work was supported by the Swiss National Science Foundation, the Swiss Priority Program MINAST, and the ‘‘Kommission zur F’orderung von Technologie und Innovation.’’ We would like to thank B. Such and F. Krok for their collaboration in the KBr(100) measurements.

\*Present address: Institut für Angewandte Photophysik, Technische Universität Dresden, D-01062 Dresden, Germany.

†Author to whom correspondence should be sent. Email address: roland.bennewitz@unibas.ch

<sup>1</sup>R. Bennewitz, T. Gyalog, M. Guggisberg, M. Bammerlin, E. Meyer, and H.-J. Güntherodt, Phys. Rev. B **60**, R11 301 (1999).

<sup>2</sup>E. Gnecco, R. Bennewitz, T. Gyalog, C. Loppacher, M. Bammerlin, E. Meyer, and H. Güntherodt, Phys. Rev. Lett. **84**, 1172 (2000).

<sup>3</sup>W. Denk and D. Pohl, Appl. Phys. Lett. **59**, 2171 (1991).

<sup>4</sup>T. Stowe, T. Kenny, D. Thomson, and D. Rugar, Appl. Phys. Lett. **75**, 2785 (1999).

<sup>5</sup>R. Lüthi, E. Meyer, M. Bammerlin, A. Baratoff, L. Howald, C. Gerber, and H.-J. Güntherodt, Surf. Rev. Lett. **4**, 1025 (1997).

<sup>6</sup>B. Gotsmann, C. Seidel, B. Anczykowski, and H. Fuchs, Phys. Rev. B **60**, 11 051 (1999).

<sup>7</sup>A. Abdurixit, A. Baratoff, and E. Meyer, Appl. Surf. Sci. **157**, 355 (2000).

<sup>8</sup>M. Gauthier and M. Tsukada, Phys. Rev. B **60**, 11 716 (1999).

<sup>9</sup>S. Jarvis, H. Yamada, K. Kobayashi, A. Toda, and H. Tokumoto, Appl. Surf. Sci. **157**, 314 (2000).

<sup>10</sup>M. Guggisberg, M. Bammerlin, C. Loppacher, O. Pfeiffer, A. Abdurixit, V. Barwich, R. Bennewitz, A. Baratoff, E. Meyer, and H.-J. Güntherodt, Phys. Rev. B **61**, 11 151 (2000).

<sup>11</sup>C. Loppacher, M. Bammerlin, F. Battiston, M. Guggisberg, D. Müller, H. Hidber, R. Lüthi, E. Meyer, and H.-J. Güntherodt, Appl. Phys. A: Mater. Sci. Process. **66**, 215 (1998).

<sup>12</sup>J. Cleveland, B. Anczykowski, A. Schmid, and V. Elings, Appl. Phys. Lett. **72**, 2613 (1998).

<sup>13</sup>F. Giessibl, Phys. Rev. B **56**, 16 010 (1997).

<sup>14</sup>C. Loppacher, M. Bammerlin, M. Guggisberg, S. Schär, R. Bennewitz, A. Baratoff, E. Meyer, and H.-J. Güntherodt, Phys. Rev. B (to be published).

<sup>15</sup>M. Guggisberg, M. Bammerlin, A. Baratoff, R. Lüthi, C. Loppacher, F. Battiston, J. Lü, R. Bennewitz, E. Meyer, and H.-J. Güntherodt, Surf. Sci. **461**, 255 (2000).

<sup>16</sup>R. Bennewitz, A. Foster, L. Kantorovich, M. Bammerlin, C. Loppacher, S. Schär, M. Guggisberg, E. Meyer, H.-J. Güntherodt, and A. Shluger, Phys. Rev. B **62**, 2074 (2000).

<sup>17</sup>B. Such, P. Czuba, P. Piatkowski, and M. Szymonski, Surf. Sci. **451**, 203 (2000).

<sup>18</sup>G. Cross, A. Schirmeisen, A. Stalder, P. Grütter, M. Tschedy, and U. Dürig, Phys. Rev. Lett. **80**, 4685 (1998).

<sup>19</sup>V. Barwich, M. Bammerlin, A. Baratoff, R. Bennewitz, M. Guggisberg, C. Loppacher, O. Pfeiffer, E. Meyer, H.-J. Güntherodt, J. Salvétat, J. Bonard, and L. Forro, Appl. Surf. Sci. **157**, 269 (2000).